CENTRE DE RECERCA MATEMÀTICA

Title:	*Optimising the heat balance integral method in spherical and cylindrical Stefan problems*
Journal Information:	*Applied Mathematics and Computation*,
Author(s):	Ribera H., Myers T.G., MacDevette M.M..
Volume, pages:	*354 16*, DOI:[10.1016/j.amc.2019.02.039]

Applied Mathematics and Computation 354 (2019) 216–231

Contents lists available at ScienceDirect

Applied Mathematics and Computation

journal homepage: www.elsevier.com/locate/amc

Optimising the heat balance integral method in spherical and cylindrical Stefan problems

H. Ribera[a,b,*], T.G. Myers[a,b], M.M. MacDevette[c]

[a] Centre de Recerca Matemàtica, Campus de Bellaterra, Edifici C, 08193 Bellaterra, Barcelona, Spain
[b] Department de Matemàtica Aplicada, Universitat Politècnica de Catalunya, Barcelona, Spain
[c] Centre for Research in Computational and Applied Mathematics, University of Cape Town, South Africa

ARTICLE INFO

Keywords:
Heat balance integral method
Stefan problem
Spherical coordinates
Cylindrical coordinates
Phase change

ABSTRACT

The Heat Balance Integral Method (HBIM) is generally applied to one-dimensional Cartesian heat flow and Stefan problems. The main reason for this being that solutions in spherical and cylindrical coordinates are less accurate than in Cartesian. Consequently, in this paper we examine the application of the HBIM to Stefan problems in spherical and cylindrical coordinates, with the aim of improving accuracy. The standard version as well as one designed to minimise errors will be applied on the original and transformed system. Results are compared against numerical and perturbation solutions. It is shown that for the spherical case it is possible to obtain highly accurate approximate solutions (more accurate than the first order perturbation for realistic values of the Stefan number). For the cylindrical problem the results are significantly less accurate.

1. Introduction

The Heat Balance Integral Method (HBIM) is an approximate solution method primarily applied to thermal and phase change problems. It has become popular largely due to its simplicity. For example, when solving a single heat equation the method permits the governing partial differential equation to be transformed to a first order ordinary differential equation, which may often be solved analytically. It is particularly useful in solving Stefan problems, where there exist very few practically useful solutions and generally numerical methods are required.

The HBIM was developed by Goodman [1] and is most commonly applied to problems in a Cartesian geometry. However, there exist many situations where an approximate solution method in cylindrical or spherical coordinates is required. Spherical Stefan problems are described in the context of the Earth cooling in [2], they are also important in industrial applications such as paint pigments, polishing materials and laser cladding [3,4]. Recently there has been great interest in the melting process at the nanoscale. Studies on spherical nanoparticle melting are often motivated by the development of new materials, although there are many important applications in medicine and drug delivery, see [6–8]. Phase change in cylindrical geometries is of interest in everyday applications such as icicle growth and melting, and certain thermal storage systems [10]. At the microscale solidification in a cylindrical geometry has been studied in the context of phase change microvalves and cryopreservation [11,12]. At the nanoscale there exists great interest in the formation or melting of nanowires,

* Corresponding author.
E-mail address: hribera.crm@gmail.com (H. Ribera).

https://doi.org/10.1016/j.amc.2019.02.039
0096-3003/

see [6,13,36]. Consequently, there is a clear need to develop solution techniques to complement this interest in thermal and melting problems in spherical and cylindrical geometries.

The Cartesian version of the HBIM is described in detail in a number of texts [14–17], while there are less published works dealing with the spherical or cylindrical versions [18–20]. Hill [21] summarizes techniques for analytical and series solutions for one-dimensional Stefan problems, including that of the HBIM in cylindrical and spherical coordinates. Ren [14] studies Cartesian and spherical geometries subject to a specified solidification front velocity and compares results for both one and two phase problems against numerics. In [34] a modified form of HBIM is applied to a spherically symmetric domain to determine the thermal conductivity of a nanofluid.

Various authors use the HBIM as the basis for a numerical scheme. In a series of papers Bell looked into subdividing the spatial and dependent variables in planar and cylindrical geometries, see [22,23]. This is analogous to a numerical marching scheme on the heat balance equations whose accuracy increases with increased number of subdivisions. Caldwell and Chiu [26] extended this method, working with cylindrical and spherical geometries. Their solution shows some inaccuracies for small Stefan numbers and has non-physical oscillations for coarse grids. In a separate paper they detail the necessary starting solution for their scheme. In [24,25] linear profiles are employed in the subdivision. This requires an increase in the number of subregions to improve accuracy. Mitchell [23] uses a boundary immobilisation technique together with a standard HBIM profile. This leads to highly accurate solutions with a very small number of subregions. The method does not require a separate small time solution and can be applied to realistic boundary conditions, rather than the fixed temperature condition used in most studies.

Various modifications of the HBIM have appeared in the literature, with the aim of improving the approximation. Sadoun [37] introduced the Refined Integral Method (RIM) which involves integrating the heat equation twice and simplifying the resultant integral via the standard HBIM integral. An alternative approach to the RIM, termed the ARIM, is mentioned in [38] where they point out that the resultant integral form may be simpler to deal with, especially when combined with a zero flux boundary condition. Mitchell and Myers [29,30] proposed the Combined Integral Method (CIM) which combines both HBIM and RIM. However (for standard boundary conditions) the most accurate formulation comes through the opTimal Integral Method (henceforth termed the TIM), which involves minimising the least squares error when the approximating function is substituted into the heat equation [27,28]. In [40,41] variations of the HBIM are investigated.

In the following section we will specify the basic one-dimensional, one-phase Stefan problem, to be used in the remainder of the paper. Studying the one-phase problem reduces the length of the expressions and so simplifies the analysis, making the exposition of the method clearer. We note that the one-phase formulation is known to lose energy when the phase change temperature is variable (such as with melting at the nanoscale or with supercooled fluids [9,31]). In the following we will avoid this issue by only dealing with fixed phase change temperature but the method could easily be extended to a variable temperature. In Section 3 we analyse phase change due to a fixed temperature boundary condition since this is the basic condition studied in the majority of papers. However, in reality the fixed temperature boundary condition is physically unrealistic so, in Section 4, we study the case of a Newton cooling condition.

2. Mathematical modelling

Consider a solid sphere or cylinder of initial radius $R = R_0$ which is at the melt temperature, T_m. At $t = 0$ the outer boundary temperature is increased such that melting begins and progresses inwards until the whole particle has turned to liquid. The liquid occupies the region $R(t) < r < R$, where $R(t)$ denotes the position of the melting front, and has initial condition $R(0) = R_0$. The problem is described by the standard one-phase formulation

$$\rho c \frac{\partial T}{\partial t} = \frac{k}{r^p}\frac{\partial}{\partial r}\left(r^p \frac{\partial T}{\partial r}\right), \qquad R(t) < r < R_0, \tag{1}$$

where ρ, c and k denote the density, specific heat and conductivity, respectively. We assume ρ is constant and equal in the solid and liquid phases throughout the melt process (this is not necessary for the analysis, but again we choose this to make the mathematics clearer). The choice $p = 2$ describes the heat equation in spherical coordinates. We may also examine Cartesian and cylindrical geometries by setting $p = 0,\ 1,$ respectively. The position of the interface is determined by the Stefan condition

$$\rho L_m \frac{\mathrm{d}R}{\mathrm{d}t} = -k \frac{\partial T}{\partial r}\bigg|_{r=R}, \tag{2}$$

where L_m denotes the latent heat. These equations are subject to the following boundary and initial conditions

$$T(R,t) = T_m, \qquad T(r,0) = T_m, \qquad R(0) = R_0,$$
$$\text{(a)}\ T(R_0,t) = T_H, \qquad \text{or} \qquad \text{(b)}\ -k\frac{\partial T}{\partial r}\bigg|_{r=R_0} = h(T(1,t) - T_H), \tag{3}$$

where at the outer boundary we will impose either a fixed temperature or Newton cooling condition.

Introducing the nondimensional variables

$$\hat{t} = \frac{k}{\rho c R_0^2}t, \qquad \hat{T} = \frac{T - T_m}{\Delta T}, \qquad \hat{r} = \frac{r}{R_0}, \qquad \hat{R} = \frac{R}{R_0}, \tag{4}$$

where $\Delta T = T_H - T_m$, the problem (1)–(3) may be written (dropping the hat notation) as

$$\frac{\partial T}{\partial t} = \frac{1}{r^p}\frac{\partial}{\partial r}\left(r^p \frac{\partial T}{\partial r}\right), \qquad R(t) < r < 1, \tag{5}$$

subject to

$$T(R,t) = 0, \qquad T(r,0) = 0, \qquad R(0) = 1,$$
$$\text{(a)}\ T(1,t) = 1, \qquad \text{or} \qquad \text{(b)}\ \left.\frac{\partial T}{\partial r}\right|_{r=1} = \mathrm{Nu}(1 - T(1,t)), \tag{6}$$

where $\mathrm{Nu} = (R_0 h)/k$ is the Nusselt number. The Stefan condition becomes

$$\beta \frac{\mathrm{d}R}{\mathrm{d}t} = -\left.\frac{\partial T}{\partial r}\right|_{r=R}, \qquad R(0) = 1, \tag{7}$$

where $\beta = L_m/(c\Delta T)$ is the Stefan number.

3. Fixed temperature boundary condition

The most commonly used boundary condition in the mathematical study of Stefan problems is that of a fixed temperature, $T(R_0, t) = T_H > T_m$. Hence in this section we will always apply Eq. 3(a) at the boundary. Physically it is unrealistic since it requires an infinite flux at the beginning of the melting process, however the mathematics involved is relatively simple so we begin our analysis with this case and subsequently move on to the more realistic case of a cooling condition.

3.1. Spherical Stefan problem

We begin our analysis with a study of the spherical problem in the original coordinate system, defined by Eqs. (5)–(7) with $p = 2$, and subsequently a transformed system. Results are then compared with a numerical solution.

3.1.1. HBIM formulation

All heat balance methods involve choosing a simple function (usually a polynomial) to approximate the temperature over a finite region [38]. We choose a standard form

$$T(r,t) = a(t)\left(\frac{r-R}{1-R}\right) + b(t)\left(\frac{r-R}{1-R}\right)^n + c(t). \tag{8}$$

To follow the original HBIM we now assume $n = 2$. The boundary conditions indicate $c = 0$ and $b = 1 - a$. In the Cartesian case a is a constant, in spherical co-ordinates it turns out to be a function of time. Hence the expression for T involves two unknown functions, $a(t)$ and $R(t)$. The first of the two equations to determine these unknowns is found by substitution of T into the Stefan condition (7). This leads to an ordinary differential equation

$$\beta \frac{\mathrm{d}R}{\mathrm{d}t} = -\frac{a}{1-R}. \tag{9}$$

A second equation, termed the Heat Balance Integral (HBI), comes from integrating the heat Eq. (5) over the region $r \in [R, 1]$,

$$\int_R^1 r^2 \frac{\partial T}{\partial t}\mathrm{d}r = \int_R^1 \frac{\partial}{\partial r}\left(r^2 \frac{\partial T}{\partial r}\right)\mathrm{d}r \quad \Rightarrow \quad \frac{\mathrm{d}}{\mathrm{d}t}\int_R^1 r^2 T(r,t)\mathrm{d}r = \left.\frac{\partial T}{\partial r}\right|_{r=1} - R^2 \left.\frac{\partial T}{\partial r}\right|_{r=R}. \tag{10}$$

Upon substituting the approximating function (8) into this expression we obtain

$$\frac{\mathrm{d}}{\mathrm{d}t}\left[\frac{(1-R)\left(\left(24 + \left(n^3 + 6n^2 + 11n - 18\right)a\right)R^2 + 2(1+n)\left(12 + \left(n^2 + 5n - 6\right)a\right)R\right)}{(2+n)(3+n)(1+n)} \frac{(1-R)(3(4 + (n-1)a)(1+n)(2+n))}{(2+n)(3+n)(1+n)}\right]$$
$$= -\frac{aR^4}{(1-R)}. \tag{11}$$

Since $n = 2$ is constant we may write (11) as

$$\frac{\mathrm{d}}{\mathrm{d}t}\left[\frac{1}{20}(1-R)\left(\left(\frac{2}{3} + a\right)R^2 + \left(\frac{4a}{3} + 2\right)R + 4 + a\right)\right] = -\frac{aR^4}{(1-R)}. \tag{12}$$

The initial condition for the melt front $R(0) = 1$ is known, but the condition for a is not. The classical Neumann solution for Cartesian phase change driven by a constant temperature boundary condition shows $R \sim \sqrt{t}$. The current problem, which describes spherical melting, (5)–(7), reduces to the Neumann problem provided the melt region is small compared to the radius. Hence, for small times, we may approximate the moving boundary position as

$$R \approx 1 - 2\lambda t^{1/2}, \tag{13}$$

where λ is an unknown constant. For the spherical problem this form has been used in [5]. Substituting this, and the derivative of T into the Stefan condition (9) determines

$$a \approx \frac{\beta\lambda^2}{2}(1 - 2\lambda t^{1/2}), \tag{14}$$

hence,

$$a(0) = \frac{\beta\lambda^2}{2}. \tag{15}$$

To find the value for λ we substitute the small time solutions (13), (15) into the heat balance (11), which in the limit $t \to 0$ gives a quadratic for λ^2

$$2\beta(n-1)\lambda^4 + (2\beta n + 2 + 2\beta n^2)\lambda^2 - n^2 - n = 0. \tag{16}$$

The standard HBIM solution to the Stefan problem is now described by Eqs. (9) and (11) with $n = 2$. The numerical solution of (9), (11), subject to $R(0) = 1$, $a(0) = \beta\lambda^2/2$ can easily be found using the ODE solver `ode45` in MATLAB.

3.1.2. TIM formulation

The standard HBIM of Goodman [1] simply imposed $n = 2$, as in the previous section, although there are many other possibilities, often chosen through knowledge of an exact solution, see [29]. The opTimal Integral Method (TIM) was developed so that n is chosen to improve the accuracy of the standard method without the need for an exact or numerical solution [27,28]. This involves minimising a least-squares error. Thus a third equation is introduced

$$E_n(r,t) = \int_R^1 \left(\frac{\partial T}{\partial t} - \frac{2}{r}\frac{\partial T}{\partial r} - \frac{\partial^2 T}{\partial r^2} \right)^2 \mathrm{d}r. \tag{17}$$

This approach has a number of advantages, the most obvious is that it significantly improves accuracy, for certain boundary conditions by orders of magnitude [27,28]. It also provides a measure of the error without knowledge of an exact solution. The algebra involved in the integral may be complex, which has been quoted as a drawback [3]. However, it is unnecessary to carry out the algebra every time the method is used. For standard Cartesian thermal problems in a fixed domain: for a constant temperature boundary condition the appropriate value is $n = 2.235$, while for constant flux and Newton cooling boundary conditions $n = 3.584$, see [28]. The Stefan problem with a fixed temperature boundary condition gives $n = 1.79$; with constant flux or a Newton cooling condition, $n = 3.48$.

The TIM formulation is fully specified by Eqs. (9), (11) and (17) for the 3 unknowns a, n, R, subject to the temperature profile (8).

As in the standard HBIM we solve (9) and (11) numerically, but now for a range of n. The error E_n is then calculated to determine the minimum value and corresponding value of n. It turns out that the optimal n varies with β. For $\beta \in [1, 10]$ we find $n \in [1.73, 1.77]$. As we will see later, the average value is accurate over a wide range of β, so effectively with a fixed temperature condition the TIM requires solving the two ODEs (9), (11) with $n = 1.75$.

3.1.3. Perturbation solution

Perhaps the most popular method for finding approximate solutions to Stefan problems is via the large Stefan number perturbation. This involves assuming that $\beta \gg 1$, although this limit is not always of practical interest: in [32, Chap 2.1] typical parameter values for the phase change of water, copper, paraffin wax and silicon dioxide are provided, these show $\beta \in [2 \times 10^{-3}, 8.3]$ (note their Stefan number $St = 1/\beta$).

The $\beta \gg 1$ limit corresponds to slow melting and requires time to be rescaled such as $\tau = \epsilon t$, where $\epsilon = 1/\beta$. Now the problem statement becomes

$$\epsilon\frac{\partial T}{\partial \tau} = \frac{1}{r^2}\frac{\partial}{\partial r}\left(r^2 \frac{\partial^2 T}{\partial r^2} \right), \qquad R(\tau) < r < 1, \tag{18}$$

$$T(R,\tau) = 0, \qquad T(1,\tau) = 1, \tag{19}$$

$$\frac{\mathrm{d}R}{\mathrm{d}\tau} = -\left.\frac{\partial T}{\partial r}\right|_{r=R}. \tag{20}$$

We then approximate the solution for T by a power series in the small parameter ϵ, $T(r,\tau) = T_0 + \epsilon T_1 + \mathcal{O}(\epsilon^2)$. Applying this expansion to the governing Eq. (18) and grouping terms with the same power of ϵ we find the leading and first order temperatures to be

$$T_0 = \frac{r - R}{(1 - R)}, \tag{21}$$

$$T_1 = -\frac{(r-1)(R-2+r)(R-r)}{6(1-R)^2}\frac{\mathrm{d}R}{\mathrm{d}\tau}. \tag{22}$$

Substituting the first order approximation of T into the Stefan condition (20) gives

$$\frac{\mathrm{d}R}{\mathrm{d}\tau} = -\frac{3}{(1-R)(3R+\epsilon)}. \tag{23}$$

Eq. (23) can easily be solved via MATLAB's `ode45`, with initial condition $R(0) = 1$. We may also easily integrate this expression to find an implicit solution for R (a cubic equation in R), but when solving the cubic numerically there is a jump in roots so we prefer to use the ODE solver.

3.1.4. Approximate solutions in the transformed system

The equations for the transformed system come from making the change $u = Tr$. The problem then becomes

$$\frac{\partial u}{\partial t} = \frac{\partial^2 u}{\partial r^2}, \qquad R < r < 1, \tag{24}$$

$$u(R,t) = 0 = u(r,0), \qquad u(1,t) = 1 \qquad R(0) = 1 \tag{25}$$

$$\beta R\frac{\mathrm{d}R}{\mathrm{d}t} = -\left.\frac{\partial u}{\partial r}\right|_{r=R}. \tag{26}$$

To approximate the temperature over a finite region we choose the standard form of Eq. (8), and replace T by u. The boundary conditions again determine $c = 0$ and $b = 1 - a$. As before we use the Stefan condition and the HBI to define equations for R and a. The Stefan condition gives

$$\beta R\frac{\mathrm{d}R}{\mathrm{d}t} = -\frac{a}{1-R}. \tag{27}$$

The heat balance integral is

$$\int_R^1 \frac{\partial u}{\partial t}\mathrm{d}r = \int_R^1 \frac{\partial^2 u}{\partial r^2}\mathrm{d}r \quad \Rightarrow \quad \frac{\mathrm{d}}{\mathrm{d}t}\int_R^1 u(r,t)\mathrm{d}r = \left.\frac{\partial u}{\partial r}\right|_{r=1} - \left.\frac{\partial u}{\partial r}\right|_{r=R}. \tag{28}$$

Upon substituting the approximating function u into this expression and assuming constant n, we obtain

$$(n-1)(1-R)^2\frac{\mathrm{d}a}{\mathrm{d}t} - (1-R)[(n-1)a+2]\frac{\mathrm{d}R}{\mathrm{d}t} = 2n(n+1)(1-a). \tag{29}$$

To find λ we again let $t \to 0$ and substitute into the HBIM (28). The solution to the Stefan problem is now described by Eqs. (27) and (29) subject to initial conditions $R(0) = 1$, $a(0) = 2\beta\lambda^2$.

In the transformed system the TIM solution requires finding the value for n that minimises the error

$$E_n(n,t) = \int_R^1 \left(\frac{\partial u}{\partial t} - \frac{\partial^2 u}{\partial r^2}\right)^2 \mathrm{d}r. \tag{30}$$

As before we simply solve the ODEs (26), (29) numerically for a range of n and then determine the value that minimises (30). We find that for $\beta \in [1,10]$, $n \in [1.55, 1.65]$, so in general we choose $n = 1.6$.

The leading and first order perturbation solutions are

$$u_0 = rT_0, \qquad u_1 = rT_1 \tag{31}$$

where T_0, T_1 are given by (21), (22), and the melt front is described by (23). That is, the perturbation solution in the transformed system is identical to that of the original system.

3.1.5. Numerical solution

To ascertain the accuracy of the various solutions we will now formulate a numerical solution. To do this, we employ a finite difference scheme, following the work of Font et al. [5]. There are two key steps: the first one consists of changing the temperature variable to $u = rT$; the second involves introducing a new coordinate to immobilise the boundary, $\eta = (r-R)/(1-R)$. This transforms the problem to

$$(1-R)^2\frac{\partial u}{\partial t} = (1-R)(1-\eta)\frac{\partial u}{\partial \eta}R_t + \frac{\partial^2 u}{\partial \eta^2}, \qquad 0 < r < 1, \tag{32}$$

$$u(0,t) = 0, \qquad u(1,t) = 1, \tag{33}$$

$$\beta R\frac{\mathrm{d}R}{\mathrm{d}t} = -\frac{1}{1-R}\frac{\partial u}{\partial \eta}\bigg|_{\eta=0}. \tag{34}$$

In the equations above, both R and R_t are evaluated at the n-th time step. We find R_t^n via Eq. (34) and approximate the partial derivative of the temperature at the boundary $\eta = 0$ via a three-point forward difference [39]. We use standard finite differences to approximate the temperature derivatives,

$$\frac{\partial u}{\partial t} = \frac{u_i^{n+1} - u_i^n}{\Delta t}, \qquad \frac{\partial u}{\partial \eta} = \frac{u_{i+1}^{n+1} - u_{i-1}^{n+1}}{2\Delta \eta}, \qquad \frac{\partial^2 u}{\partial \eta^2} = \frac{u_{i+1}^{n+1} - 2u_i^{n+1} + u_{i-1}^{n+1}}{\Delta \eta^2}, \tag{35}$$

where $i = 1, \ldots, J$ and $n = 1, \ldots, N$. Hence we may write

$$u_i^{n+1} = 0, \qquad i = 1, \tag{36}$$

$$a_i^n u_{i-1}^{n+1} + b_i^n u_i^{n+1} + c_i^n u_{i+1}^{n+1} = d^n u_i^n, \qquad i = 2, \ldots, J-1, \tag{37}$$

$$u_i^{n+1} = 1, \qquad i = J, \tag{38}$$

which allows us to write down a matrix system that we solve at every time step n. We determine the position of the melt front via the Stefan condition (34) using a three-point backward difference for the partial derivative, and taking the time derivative to be

$$\frac{\mathrm{d}R}{\mathrm{d}t} = \frac{R^{n+1} - R^n}{\Delta t}. \tag{39}$$

Small time analysis

A common difficulty when solving Stefan problems numerically is that the liquid phase does not exist at $t = 0$, however a numerical solution demands initial values. To overcome this difficulty we look for a small time solution to provide an initial guess within the numerical scheme. As stated earlier, at small times $R = 1 - 2\lambda t^{1/2}$, substituting this into Eq. (32) and letting $t \to 0$ gives

$$\frac{\partial^2 u}{\partial \eta^2} \approx 0. \tag{40}$$

Applying the boundary condition (33) yields $u(\eta, t) = \eta$. Substituting this expression into the Stefan condition (34) allows us to find $\lambda = \sqrt{1/(2\beta)}$. So we start our scheme at some time $t = t_0 \ll 1$, with $u(\eta, t_0) = \eta$ and $R(t_0) = 1 - \sqrt{(2t_0)/\beta}$.

3.1.6. Comparison of results

The most important variable in the Stefan problem is the position of the melt front $R(t)$: the main reason for solving the heat equation is to find the temperature gradient which then drives the phase change. Consequently, in Fig. 1 we show a comparison of the melt front predictions of the numerical solution (solid line) and the approximate solutions in the original domain for $\beta = 1, 10$. The TIM, the HBIM with $n = 2$ and perturbation solutions are shown as dashed, dash-dotted and dotted lines, respectively. For $\beta = 1$ all solutions are inaccurate. When $\beta = 10$ the perturbation solution is very close to the numerical solution while the other solutions are again inaccurate. In Fig. 2 we show the equivalent results, but now calculated in the transformed system. For $\beta = 1$ the TIM shows reasonable agreement, with a final melt time some 7% larger than the numerical prediction. The HBIM and perturbation solutions are highly inaccurate. For $\beta = 10$ we expect the large β perturbation to be accurate, and indeed it is much closer to the numerical solution now. However, as is clear from the inset, the TIM is significantly more accurate. This is in keeping with the results of [30] where it is shown that for $\beta \in [0.1, 10]$ their heat balance method is more accurate than the second order small and large β perturbation solutions. For $\beta > 10$ both their heat balance solution and the perturbation are highly accurate, with errors below 0.01%. From these two figures we can conclude that in spherical co-ordinates the most accurate solution is generally obtained via the TIM, that is with $n = 1.6$, in the transformed system.

In Fig. 3(a) we show temperature profiles for different times as a function of r for $\beta = 1$ for the different methods presented, in the transformed system. We observe that for early times the temperatures for all different methods are very similar, but as time increases the agreement diminishes considerably. There are two main factors that contribute to this. The first one, of course, is the difference in the expressions that define the temperatures. But the most important factor is the fact that at later times, as can be seen in Fig. 2(a), the difference in the R increases, and thus the temperature profiles become even more different. To illustrate this, we plot in Fig. 3(b) the temperature profiles for the different methods using the same value (from the numerical solution) for R at the different times. We see, that despite there are still some differences, they have decreased substantially.

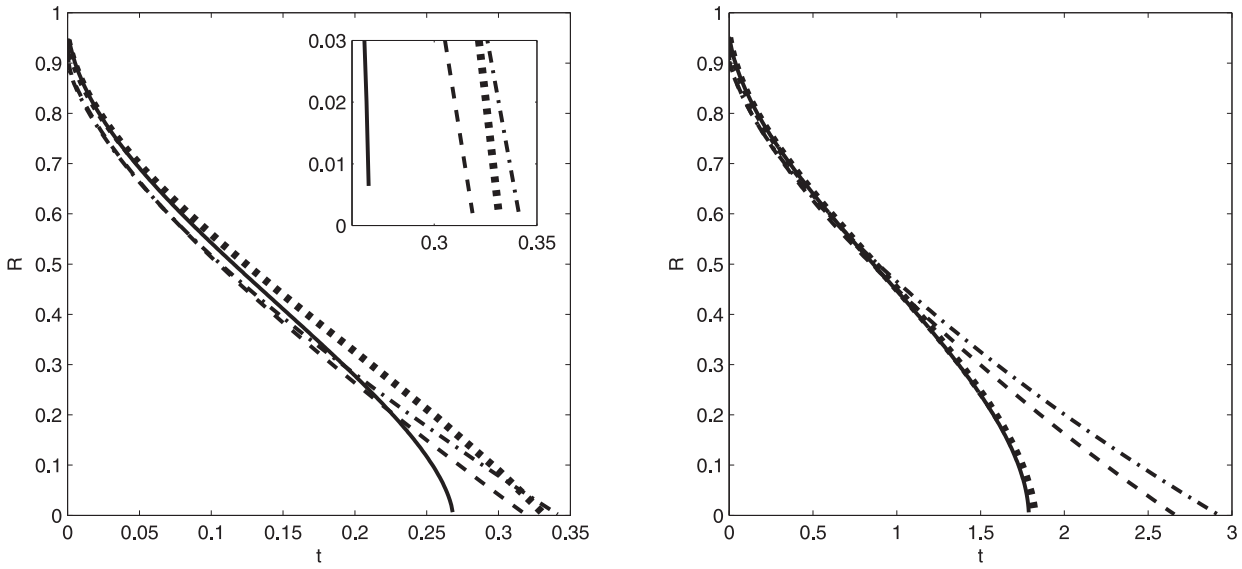

(a) $\beta = 1.$ (b) $\beta = 10.$

Fig. 1. Melting front evolution of a spherical particle in the original system for HBIM (dash-dotted), TIM (dashed), perturbation (dotted) and numerical (solid) solutions for $\beta = 1,\ 10$.

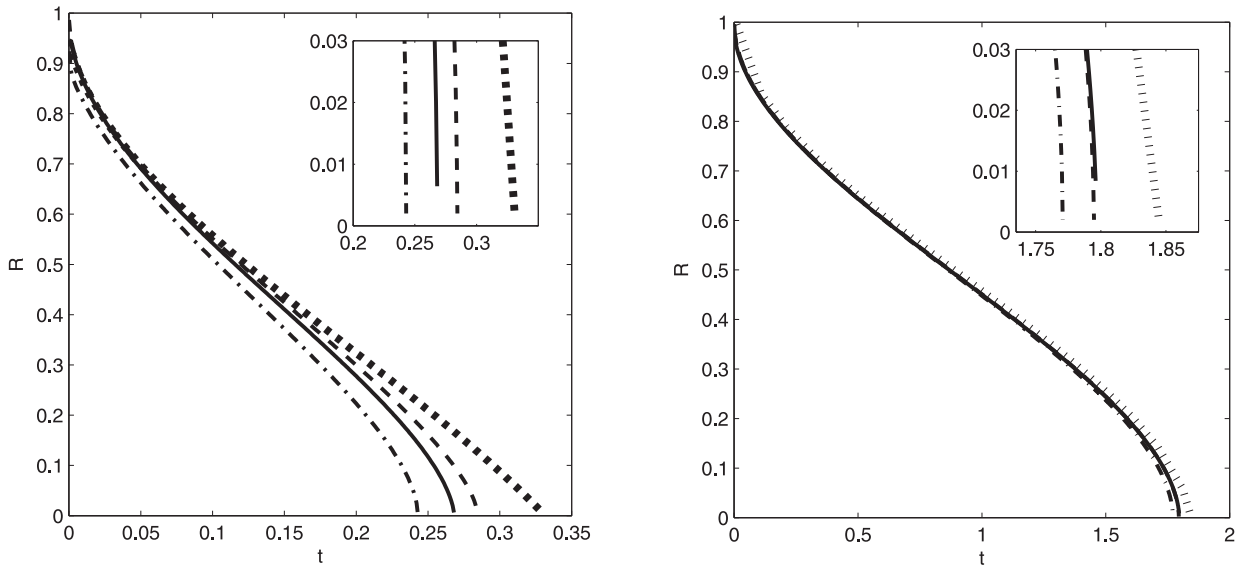

(a) $\beta = 1.$ (b) $\beta = 10.$

Fig. 2. Melting front evolution of a spherical particle in the transformed system for HBIM (dash-dotted), TIM (dashed), perturbation (dotted) and numerical (solid) solutions for various β.

3.2. Cylindrical Stefan problem

In this section we focus on the cylindrical Stefan problem. We will follow the methods outlined in the previous section and so will omit much of the detail. Again we first solve the problem in the original system, Eqs. (5)–(7) taking $p = 1$, and later on provide approximate solutions for a transformed system.

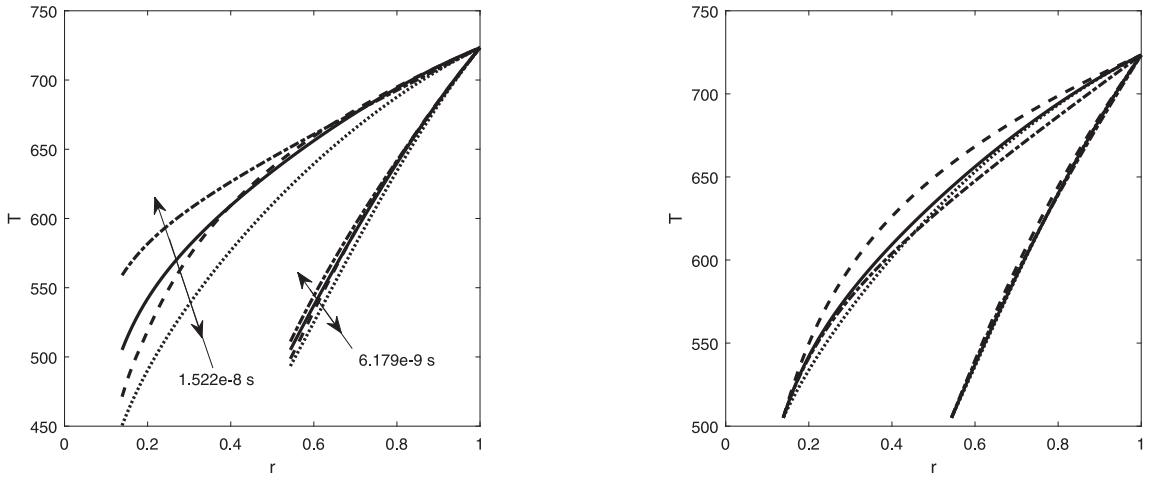

(a) Using the corresponding R values for each method. (b) Using the same R value for all methods.

Fig. 3. Temperature profile of a spherical particle using the solutions in the transformed system for HBIM (dash-dotted), TIM (dashed), perturbation (dotted) and numerical (solid) solutions. $\beta = 1$.

3.2.1. Approximate solutions in the original cylindrical coordinates

We assume a temperature profile of the form (8) where $c = 0$ and $b = 1 - a$. The heat balance integral may now be expressed as

$$\frac{\mathrm{d}}{\mathrm{d}t}\int_R^1 rT\mathrm{d}r = \left.\frac{\partial T}{\partial r}\right|_{r=1} - R\left.\frac{\partial T}{\partial r}\right|_{r=R}. \tag{41}$$

Substituting for T leads to a rather long expression for the ODE, similar to (11), so we omit it in this section.

We close the system by inserting the assumed temperature profile (8) into the Stefan condition (7), to reproduce (9). For small times, for a sufficiently thin melt region the governing equations are equivalent to the Cartesian system so again we may write $R \approx 1 - 2\lambda t^{1/2}$, $a \approx \beta\lambda^2/2$. In the limit $t \to 0$ the HBI provides an equation for λ,

$$\frac{n}{2} - \frac{1}{2}\lambda\beta n = \frac{\lambda}{8(n+1)(4+\beta\lambda^2(n-1))}. \tag{42}$$

For the standard HBIM we substitute $n = 2$ to determine $\lambda(\beta)$. For the TIM, n is chosen to minimise the error function (calculated using MATLAB)

$$E(n,t) = \int_R^1 \left(\frac{\partial T}{\partial t} - \frac{1}{r}\frac{\partial T}{\partial r} - \frac{\partial^2 T}{\partial r^2}\right)^2 \mathrm{d}r. \tag{43}$$

Numerical integration of the above gives $n \in [1.404, 1.6869]$ as the optimal choice for $\beta \in [1, 10]$.

For the perturbation solution we rescale time and expand the temperature in powers of ϵ to find the leading and first order solutions

$$T_0(r,t) = 1 - \frac{\ln(r)}{\ln(R)}, \tag{44}$$

$$T_1(r,t) = \frac{((R^2 - r^2)\ln(r) + r^2 - 1)\ln(R) + (1 - R^2)\ln(r)}{4R\ln(R)^3}\frac{\mathrm{d}R}{\mathrm{d}t}. \tag{45}$$

Upon substitution into the Stefan condition, the melt front satisfies

$$\frac{\mathrm{d}R}{\mathrm{d}t} = -\frac{4\beta R\ln(R)^2}{4\beta R^2\ln(R)^3 + 2R^2\ln(R)^2 - 2R^2\ln(R) + (R^2 - 1)}, \tag{46}$$

with $R(0) = 1$.

3.2.2. Approximate solutions in a transformed system

The transformation $u = rT$ does not help in this case. Instead we follow [21,33] and use the following boundary fixing transformation,

$$\rho = \frac{\ln(r)}{\ln(R)}, \quad \tau = \ln(R), \quad T(r,t) = u(\rho,\tau). \tag{47}$$

The cylindrical problem becomes

$$e^{-2\tau\rho}\frac{\partial^2 u}{\partial \rho^2} = \tau\frac{\mathrm{d}\tau}{\mathrm{d}t}\left(\tau\frac{\partial u}{\partial \tau} - \rho\frac{\partial u}{\partial \rho}\right), \quad \rho \in [0,1], \quad \tau < 0 \tag{48}$$

$$u(1,\tau) = 1, \quad \text{(a) } u(0,\tau) = 1 \qquad \tau(0) = 0, \tag{49}$$

$$\left.\frac{\partial u}{\partial \rho}\right|_{\rho=1} = -\beta e^{2\tau}\tau\frac{\mathrm{d}\tau}{\mathrm{d}t}. \tag{50}$$

To remove the t dependence in Eq. (48) we may substitute for τ_t from the Stefan condition.

This transformation complicates the heat equation, with the result that if we leave n unknown the HBI cannot be integrated analytically, hence we cannot specify one of the ODEs for the TIM solution. However, we may still make progress for the particular case $n = 2$.

The quadratic polynomial satisfying boundary conditions (49) is

$$u(\rho,\tau) = 1 - (1+a)\rho + a\rho^2. \tag{51}$$

where $a = a(\tau)$. The HBI is obtained by integrating the heat Eq. (48) over the domain $\rho \in [0, 1]$, after removing the t dependence via the Stefan condition. This leads to

$$\int_0^1 \beta\frac{\partial^2 u}{\partial \rho^2}\mathrm{d}\rho = \int_0^1 e^{2\tau(\rho-1)}(a-1)\left[\rho\frac{\partial u}{\partial \rho} - \tau\frac{\partial u}{\partial \tau}\right]\mathrm{d}\rho. \tag{52}$$

Applying u from (51) leads to the ODE for $a(\tau)$,

$$\frac{\mathrm{d}a}{\mathrm{d}\tau} = \frac{e^{-2\tau}\left(a^2(\tau+2) - 2a - \tau\right) + 8\beta a\tau^3 - 2\tau^2(a-1)^2 + (1+3a^2-4a)\tau + 2a(1-a)}{\tau(a-1)((\tau+1)e^{-2\tau} + \tau - 1)}. \tag{53}$$

Note, unlike in previous examples we now only have a single equation to solve for $a(\tau)$, although again we do not know the initial condition. To find the value of $a(0)$ we apply the small time solution $\tau = \ln(R) = \ln(1 - 2\lambda t^{1/2})$ to the Stefan condition (50). Taking the limit $t \to 0$ gives

$$a(0) = 1 - 2\lambda^2\beta. \tag{54}$$

Substituting for a, τ into (53) leads to a quadratic for λ,

$$\frac{1}{3}\lambda^4\beta^2 + \left(\frac{\beta}{3} + 2\beta^2\right)\lambda^2 - \beta = 0. \tag{55}$$

Now we simply have to solve (53) numerically over the range $\tau \in [0, -\infty]$ subject to (54). With this transformation the melt front is at $R = e^{\tau}$. Once a is known we can convert from τ to t by solving the Stefan condition (50)

$$\frac{\mathrm{d}\tau}{\mathrm{d}t} = -\frac{a-1}{\beta}e^{2\tau} \tag{56}$$

In practice we calculate t via the discretisation

$$t_i = t_{i-1} - \frac{\beta\tau_{i-1}e^{2\tau_{i-1}}}{a_{i-1} - 1}(\tau_i - \tau_{i-1}) \tag{57}$$

where $t_0 = 0$.

With a large Stefan number we rescale time scale to obtain

$$\epsilon\tau\frac{\mathrm{d}\tau}{\mathrm{d}t}\left(\tau\frac{\partial u}{\partial \tau} - \rho\frac{\partial u}{\partial \rho}\right) = e^{-2\tau\rho}\frac{\partial^2 u}{\partial \rho^2}, \qquad 0 < \rho < 1, \tag{58}$$

$$\left.\frac{\partial u}{\partial \rho}\right|_{\rho=1} = -e^{2\tau}\tau\frac{d\tau}{dt}. \tag{59}$$

subject to (49). This leads to

$$u_0 = 1 - \rho, \tag{60}$$

$$u_1 = -\frac{(1-\rho\tau)e^{2\rho\tau} + \rho e^{2\tau}(\tau - 1) - 1 + \rho}{4\tau^2}\frac{\mathrm{d}\tau}{\mathrm{d}t}. \tag{61}$$

Finally, we find that the melt front is given by the same expression as in (46).

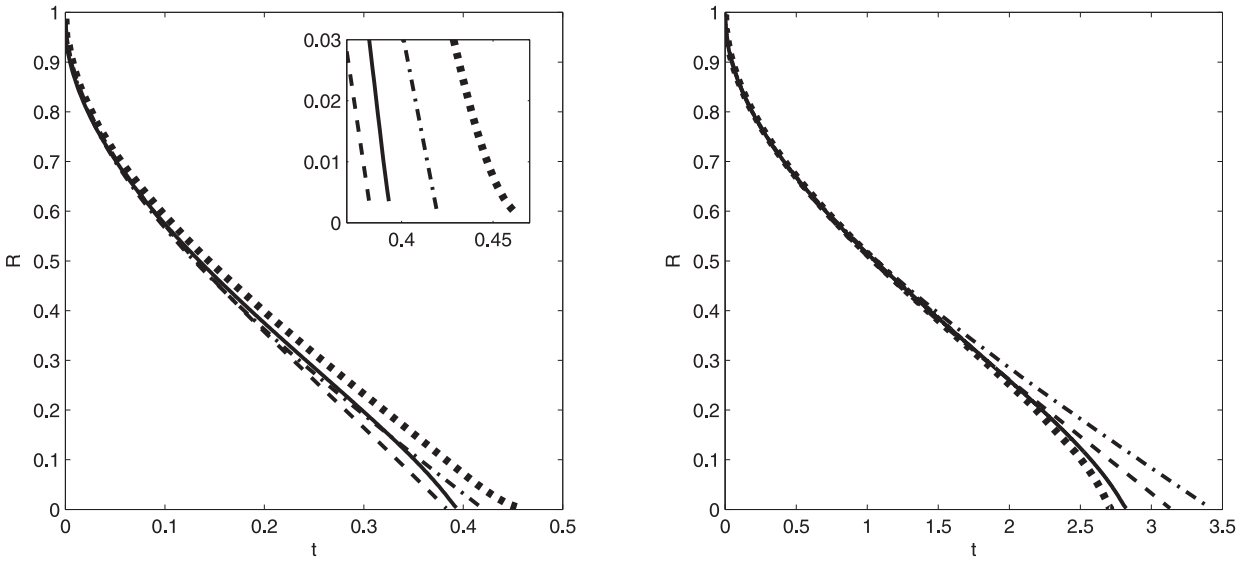

Fig. 4. Melting front evolution of a cylindrical particle in the original system for HBIM (dash-dotted), TIM (dashed), perturbation (dotted) and numerical (solid) solutions for various β.

3.2.3. Numerical solution

To solve the cylindrical problem numerically we immobilise the boundary as in the spherical case via the coordinate $\eta = (r - R)/(1 - R)$. The governing Eqs. (5)–(7) transform to

$$(1-R)^2 \frac{\partial T}{\partial t} = \left((1-\eta)(1-R)\frac{\mathrm{d}R}{\mathrm{d}t} + \frac{1-R}{\eta(1-R)+R} \right) \frac{\partial T}{\partial \eta} + \frac{\partial^2 T}{\partial \eta^2}, \tag{62}$$

$$T(0,t) = 0, \qquad T(1,t) = 1, \tag{63}$$

$$\beta(1-R)\frac{\mathrm{d}R}{\mathrm{d}t} = -\frac{\partial T}{\partial \eta}\Big|_{\eta=0}. \tag{64}$$

We use standard finite differences to approximate the temperature derivatives as in (35). As in the spherical case, we can now write

$$T_i^{n+1} = 0, \qquad i = 1, \tag{65}$$

$$\hat{a}_i^n T_{i-1}^{n+1} + \hat{b}_i^n T_i^{n+1} + \hat{c}_i^n T_{i+1}^{n+1} = \hat{d}^n T_i^n, \qquad i = 2, \ldots, J-1, \tag{66}$$

$$T_i^{n+1} = 1, \qquad i = J, \tag{67}$$

which allows us to write down a matrix system that we solve at every time step n. We are able to determine the position of the melt front via the Stefan condition (64) using a three-point backward difference for the partial derivative, and taking the time derivative to be (39). The small time analysis leads to $R \approx 1 - 2\lambda t^{1/2}$, with $\lambda = \sqrt{1/(2\beta)}$.

3.2.4. Comparison of results

In Fig. 4 we present the numerical and approximate solutions in the original domain for $\beta = 1$, 10. In this case all the heat balance methods are inaccurate for approximately $R < 0.3$. As expected the perturbation solution is poor for $\beta = 1$ and much more accurate when $\beta = 10$. In both cases the TIM is more accurate than the standard HBIM but neither is sufficiently accurate to justify their use.

In Fig. 5 we show a comparison of the melt front predictions of the numerical solution (solid line) and the approximate solutions in the transformed domain for various β. The HBIM with $n = 2$ and perturbation solutions are shown as dash-dotted and dotted lines, respectively. At small times all solutions agree well, however as R decreases they begin to diverge.

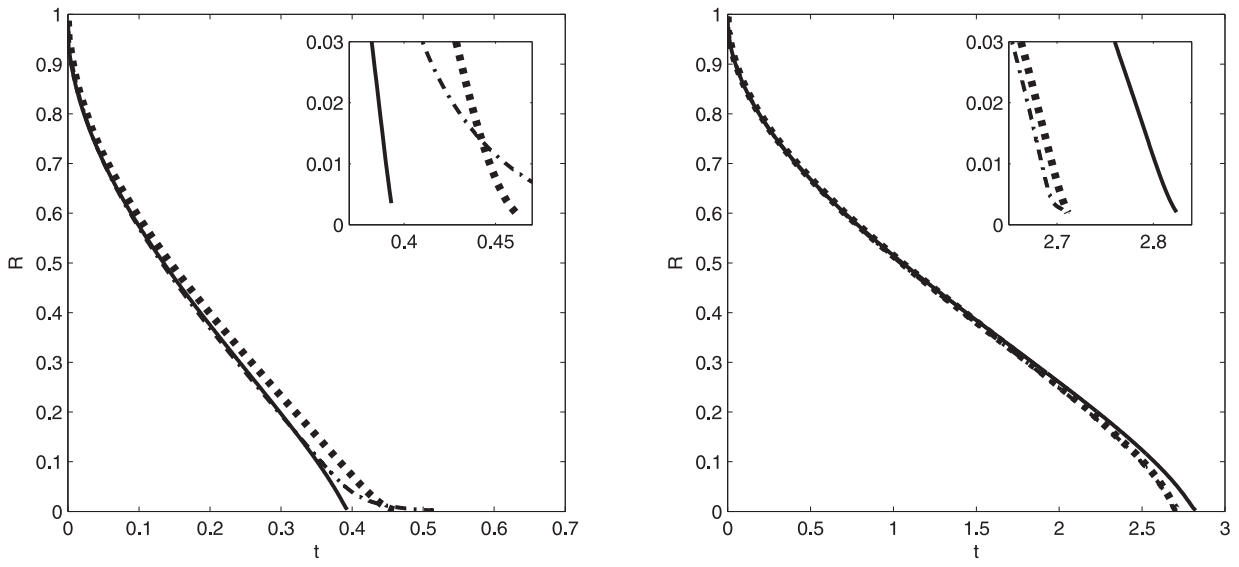

Fig. 5. Melting front evolution of a cylindrical particle in the transformed system for HBIM (dash-dotted), perturbation (dotted) and numerical (solid) solutions for various β.

For the case where $\beta = 1$, shown in Fig. 5(a), we see that the HBIM and perturbation both present errors of about 10%. In Fig. 5(b) we present results for $\beta = 10$. Now the solutions are more accurate, with the same error of about 3.5%.

4. Newton cooling boundary condition

In practice a fixed temperature boundary condition is difficult to maintain; a fixed flux or Newton cooling condition is more physically realistic [35]. We now focus on the Newton cooling condition, which means using boundary condition (3b). Again, since we follow the methods of the previous section we omit most details.

4.1. Spherical problem

The problem is specified by (5) and (6), with $p = 2$, and the Newton cooling boundary condition (b). The polynomial to approximate the temperature T is given by (8), but now $c = 0$ and $b = \frac{\mathrm{Nu}(1-R)(a-1)+aR}{(1-\mathrm{Nu})(1-R)-n}$. The heat balance integral is given by (11), which upon substituting for T from (8), with the corresponding c and b yields

$$\frac{\mathrm{d}}{\mathrm{d}t}\left[\frac{a}{1-R}\left(\frac{1}{2}-R\right)+\frac{1-R}{n+1}\left(\frac{[-\mathrm{Nu}-a(1-\mathrm{Nu})](1-R)+a}{(1-\mathrm{Nu})(1-R)-n}\right)+\frac{aR^2}{2(1-R)}\right] = \frac{n}{1-R}\left(\frac{[-\mathrm{Nu}-a(1-\mathrm{Nu})](1-R)+a}{(1-\mathrm{Nu})(1-R)-n}\right). \tag{68}$$

The second ODE is simply the Stefan condition (9).

Small time analysis

At small times R takes the form $R \approx 1 - \lambda t$, see [35]. Substituting this into the Stefan condition determines the initial condition for $a \approx \beta\lambda^2 t$. To determine the initial conditions for the numerical solution we substitute both these small time solutions into Eq. (32), and upon letting $t \to 0$, we may write $u_{\eta\eta} \approx 0$. Applying the appropriate boundary conditions yields the small time form for u,

$$u(\eta, t) = -\frac{1-R}{(1-R)(1-\mathrm{Nu})-1}\eta. \tag{69}$$

Substituting the above expression for $u(\eta, t)$ into the Stefan condition (34) determines $\lambda = \mathrm{Nu}/\beta$.

In contrast to the previous solutions, since $\mathrm{Nu} = R_0 h/k$ there is a dependence on the initial size. The solution by the TIM shows that for $\mathrm{Nu} = 15$ and $\beta \in [1, 10]$, the optimal $n \in [2.7, 3.55]$. For $\mathrm{Nu} = 1$ there is a similarly large variation in n.

Table 1
TIM exponent for different β and Nu in the transformed system.

		TIM exponent
Nu = 1.5	$\beta = 1$	1.95
	$\beta = 10$	1.89
Nu = 15	$\beta = 1$	1.68
	$\beta = 10$	1.63

The leading and first order solutions for the perturbation are

$$T_0 = \frac{F_1}{r} + F_2, \tag{70}$$

$$T_1 = \frac{r^2}{6}\frac{\mathrm{d}F_1}{\mathrm{d}t} + \frac{r}{2}\frac{\mathrm{d}F_2}{\mathrm{d}t} + F_3 + \frac{F_4}{r}, \tag{71}$$

where

$$F_1 = \frac{\mathrm{Nu}}{R(1-\mathrm{Nu}) + \mathrm{Nu}}, \tag{72}$$

$$F_2 = -\frac{\mathrm{Nu}R}{R(1-\mathrm{Nu}) + \mathrm{Nu}}, \tag{73}$$

$$F_3 = \frac{1-\mathrm{Nu}}{\mathrm{Nu}}\left[\frac{1}{6}\frac{\mathrm{d}F_1}{\mathrm{d}t} + \frac{1}{2}\frac{\mathrm{d}F_2}{\mathrm{d}t} + F_4\right] - \frac{1}{2\mathrm{Nu}}\frac{\mathrm{d}F_1}{\mathrm{d}t} - \frac{1}{\mathrm{Nu}}\frac{\mathrm{d}F_2}{\mathrm{d}t}, \tag{74}$$

$$F_4 = -\frac{R}{6R(1-\mathrm{Nu}) + 6\mathrm{Nu}}\left[(\mathrm{Nu}R^2 - 2 - \mathrm{Nu})\frac{\mathrm{d}F_1}{\mathrm{d}t} + 3(R\mathrm{Nu} - 1 - \mathrm{Nu})\frac{\mathrm{d}F_2}{\mathrm{d}t}\right]. \tag{75}$$

Substituting the first order approximation for T into the Stefan condition leads to

$$\frac{\mathrm{d}R}{\mathrm{d}t} = -\frac{3\mathrm{Nu}[(\mathrm{Nu}-1)R - \mathrm{Nu}]^2}{\left[3\mathrm{Nu}[(\mathrm{Nu}-1)R - \mathrm{Nu}]^3 - \epsilon\mathrm{Nu}(1-R)\left(1 + \mathrm{Nu} + \mathrm{Nu}^2 + (1 + \mathrm{Nu} - 2\mathrm{Nu}^2)R + (\mathrm{Nu}-1)^2R^2\right)\right]}. \tag{76}$$

Eq. (76) can be solved via MATLAB's `ode45`.

For the transformed system, with $u = Tr$, the polynomial approximation is given by (8), with $c = 0$ and $b = \frac{\mathrm{Nu}(1-R)(a-1)+aR}{(1-\mathrm{Nu})(1-R)-n}$ and the heat balance integral is given by Eq. (28). The HBIM solution to the Stefan problem is now described by Eq. (27) for R, and substituting u into (28) we obtain an ODE for a. These two equations are subject to the initial conditions stated in the small time analysis. The TIM yields values for n that vary with β and Nu, $n \in [1.63, 1.95]$ (see Table 1).

The perturbation solution is the same in the transformed system as in the original. For the numerical solution we employ the same scheme defined in Section 3.1.5, the only difference is due to the boundary condition, so that for $i = J$, $(1 - (1-\mathrm{Nu})(1-R^n)\Delta\eta)u_i^{n+1} - u_{i-1}^{n+1} = \mathrm{Nu}(1-R^n)\Delta\eta$.

In Fig. 6 we show two results for $R(t)$ in the original system. As in the previous case we observe that for small β no approximation method is suitable. For $\beta = 10$ the perturbation solution provides reasonable accuracy, which obviously will improve as β increases. In Fig. 7 we show results in the transformed system. Now the integral methods are clearly superior, providing good agreement in all examples. Interestingly, for the case $\beta = 1$, $\mathrm{Nu} = 1.5$ we can see from the inset that the standard HBIM with $n = 2$ is more accurate than the TIM, with $n = 1.95$, although both are obviously good approximations. The reason behind this is that the TIM is based on a global minimisation of the error in the temperature. This does not guarantee the most accurate temperature gradient at $r = R$. It seems that in this case the standard HBIM better approximates the gradient, $T_r(R, t)$, (at least as $R \to 0$) better than the TIM. However, as may be seen from the other three figures, in general the TIM is most accurate. Approximate values for n are provided in Table 1. Note, as $\mathrm{Nu} \to \infty$ the Newton cooling condition tends to the fixed boundary temperature boundary condition and so $n \approx 1.6$ (as predicted previously). For small Nu, $n \approx 1.92$. For simplicity we could take $n = 1.76$ for any Nu, β and find a good approximation. For better accuracy we could derive a function which moves smoothly between the limits (1.6, 1.95) as Nu moves between 0 and ∞.

4.2. Cylindrical problem

Here we follow the method of Section 3.2. In the original coordinate system we assume that the temperature profile has the form (8), with $c = 0$ and $b = \frac{(1+\mathrm{Nu}-\mathrm{Nu}R)a - \mathrm{Nu}(1-R)}{\mathrm{Nu}R - \mathrm{Nu} - n}$. The heat balance integral may be expressed as (41). We close the

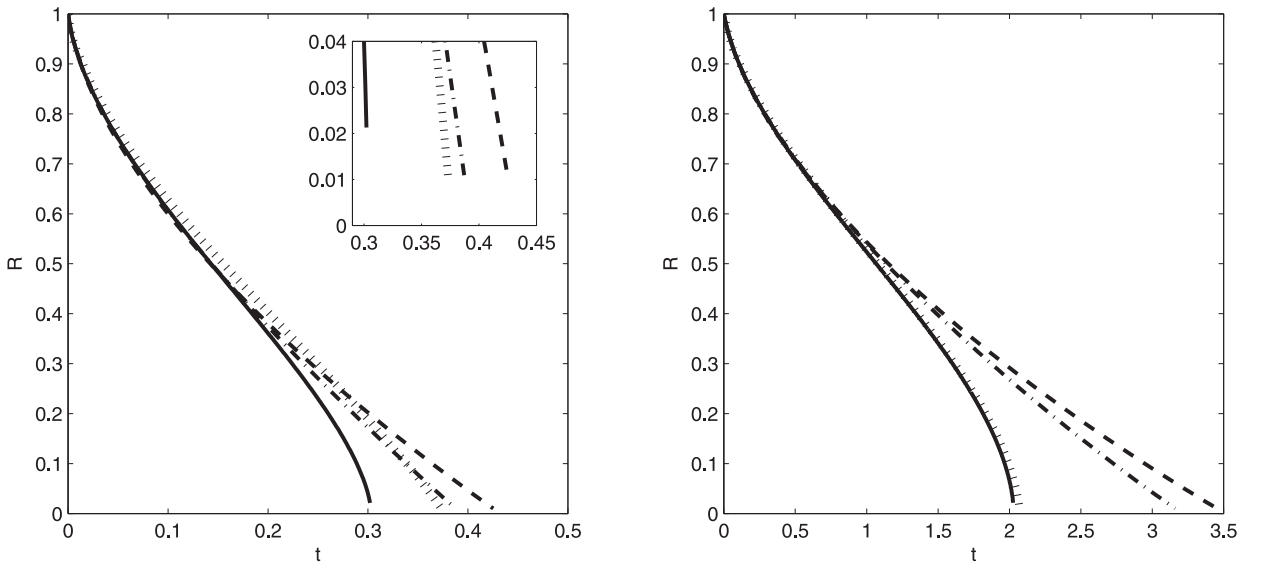

(a) $\beta = 1$, Nu $= 15$. (b) $\beta = 10$, Nu $= 15$.

Fig. 6. Melting front evolution of a spherical particle in the original system for HBIM (dash-dotted), TIM (dashed), perturbation (dotted) and numerical (solid) solutions for various β and Nu.

system by applying (8) to the Stefan condition. Assuming $R \approx 1 - \lambda t$ at small times, the Stefan condition leads to $a(0) \approx \beta\lambda^2 t$, and taking the limit $t \to 0$ in the HBI yields $\lambda = \mathrm{Nu}/\beta$. Finally, the best n is chosen to minimise the error function (43) at the final times. This gives $n \in [2.19, 2.62]$ as the optimal choice for $\beta = 1,\ 10,\ \mathrm{Nu} = 15$.

The leading and first order perturbation solutions are

$$T_0(r,t) = F_1(t) + F_2(t)\ln(r), \tag{77}$$

$$T_1(r,t) = F_3(t)\ln(r) + \frac{r^2}{4}\frac{\mathrm{d}F_1}{\mathrm{d}t} + \frac{r^2}{4}\frac{\mathrm{d}F_2}{\mathrm{d}t}\ln(r) - \frac{r^2}{4}\frac{\mathrm{d}F_2}{\mathrm{d}t} + F_4, \tag{78}$$

where

$$F_1(t) = \frac{\mathrm{Nu}\ln(R)}{\mathrm{Nu}\ln(R) - 1}, \tag{79}$$

$$F_2(t) = \frac{\mathrm{Nu}}{1 - \mathrm{Nu}\ln(R)}, \tag{80}$$

$$F_3(t) = -\frac{1}{4}\frac{\left(R^2\ln(R)\mathrm{Nu}^2 + \left(-\mathrm{Nu} - \mathrm{Nu}^2\right)R^2 + 2\,\mathrm{Nu} + \mathrm{Nu}^2 + 2\right)\mathrm{Nu}}{R(-1 + \mathrm{Nu}\ln(R))^3}\frac{\mathrm{d}R}{\mathrm{d}t}, \tag{81}$$

$$F_4(t) = \frac{1}{4}\frac{\mathrm{Nu}\left(\left(2 + 2\,\mathrm{Nu} + \mathrm{Nu}\,R^2 + \mathrm{Nu}^2\right)\ln(R) - R^2(1 + \mathrm{Nu})\right)}{R(-1 + \mathrm{Nu}\ln(R))^3}\frac{\mathrm{d}R}{\mathrm{d}t}. \tag{82}$$

The melting front is given by

$$\frac{\mathrm{d}R}{\mathrm{d}t} = \frac{4\mathrm{Nu}(\ln(R)\mathrm{Nu} - 1)^2}{\left(4\mathrm{Nu}^3\ln(R)^3 - 12\mathrm{Nu}^2\ln(R)^2 + (+12\mathrm{Nu})\ln(R) - 4\right)R}. \tag{83}$$

For the transformed system, given by the change of coordinates (47), the outer boundary condition is $\left.\frac{\partial u}{\partial \rho}\right|_{\rho=0} = \tau\lambda(1 - u(0,\tau))$. The polynomial approximation is given by

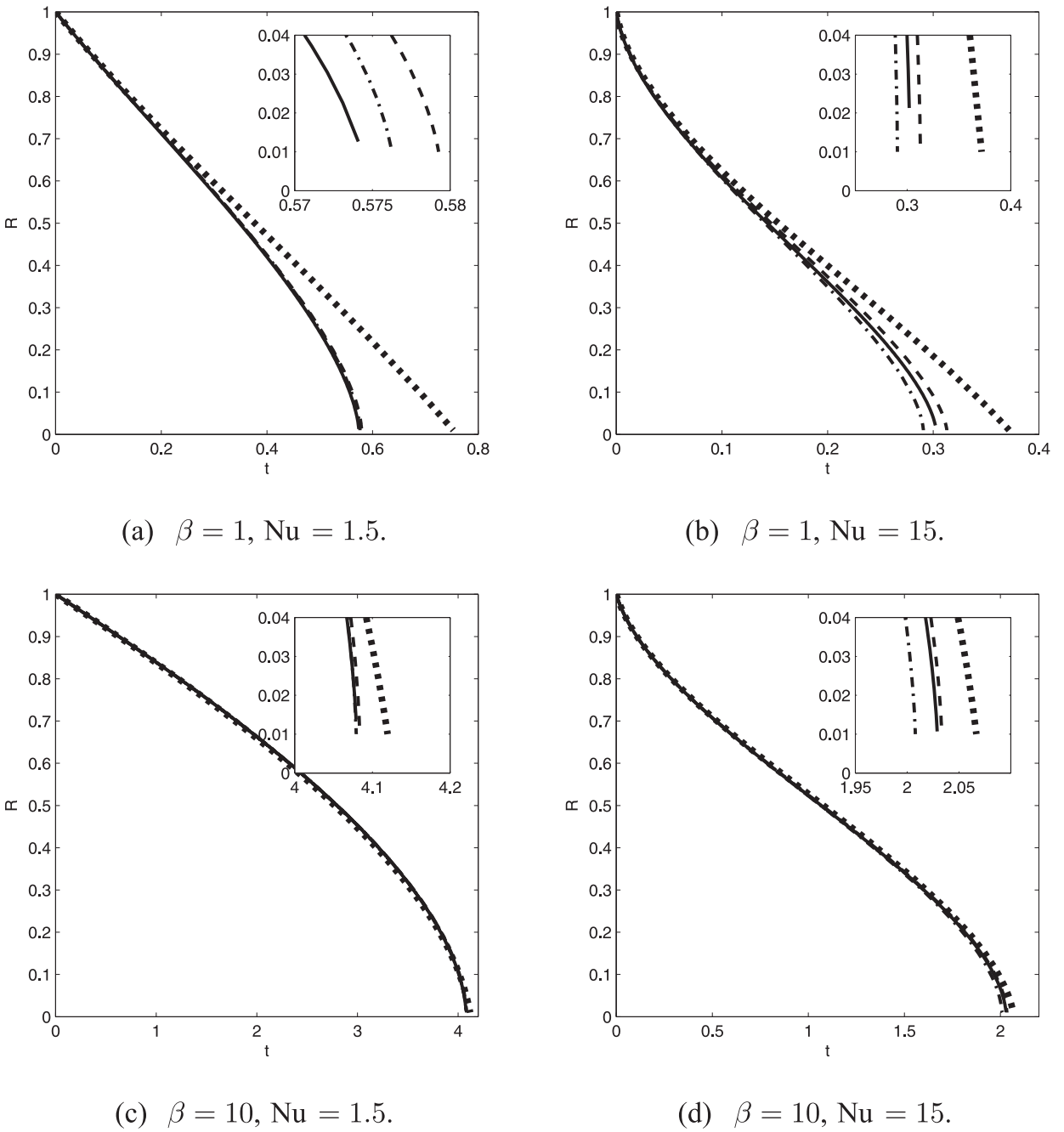

(a) $\beta = 1$, Nu $= 1.5$. (b) $\beta = 1$, Nu $= 15$.

(c) $\beta = 10$, Nu $= 1.5$. (d) $\beta = 10$, Nu $= 15$.

Fig. 7. Melting front evolution of a spherical particle in the transformed system for HBIM (dash-dotted), TIM (dashed), perturbation (dotted) and numerical (solid) solutions for various β and Nu.

$$u(\rho, \tau) = c + \tau \mathrm{Nu}(1-c)\rho - (c + \tau \mathrm{Nu}(1-c))\rho^2. \tag{84}$$

Then the heat balance integral yields

$$\frac{\mathrm{d}c}{\mathrm{d}\tau} = \frac{-2(\tau \mathrm{Nu}(c-1) - 2c)^2 \mathrm{e}^{-2\tau}\left(1/2 + \tau^2 - \tau\right)\mathrm{e}^{2\tau} + ((\tau \mathrm{Nu} - 2)c - \tau\,\mathrm{Nu})^2 \mathrm{e}^{-2\,\tau} + 8\beta\tau^3(\tau \mathrm{Nu}(c-1) - c)}{(-\tau \mathrm{Nu} + \tau \mathrm{Nu}c - 2c)\left(\left(1 + \tau^2 \mathrm{Nu} + (-2 - \mathrm{Nu})\tau\right)\mathrm{e}^{2\tau} - 1 + (2 + \mathrm{Nu})\tau^2 + \tau \mathrm{Nu}\right)\mathrm{e}^{-2\tau}\tau}. \tag{85}$$

The small time solution is $c(0) = 1 - 2\beta\lambda^2$. Now (85) is solved numerically using an ODE solver in MATLAB over the range $[0, -\infty]$. The corresponding melt front is simply $R = e^{\tau}$. We use (57) to convert the interval from τ back to t. For the perturbation solution, we find that the melt front is given by (83).

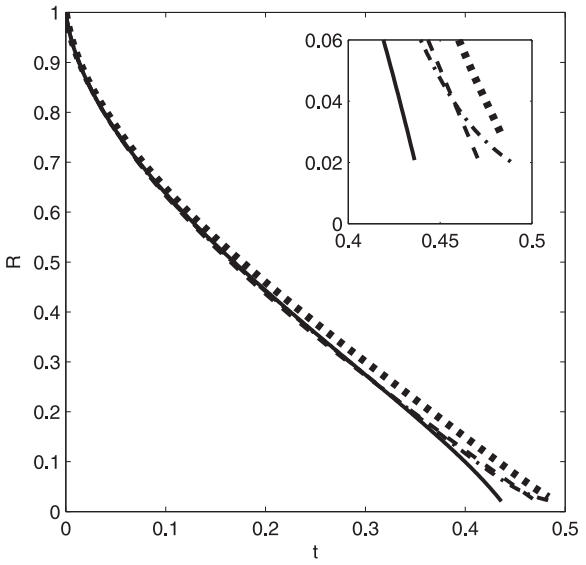

(a) $\beta = 1$, Nu $= 15$.

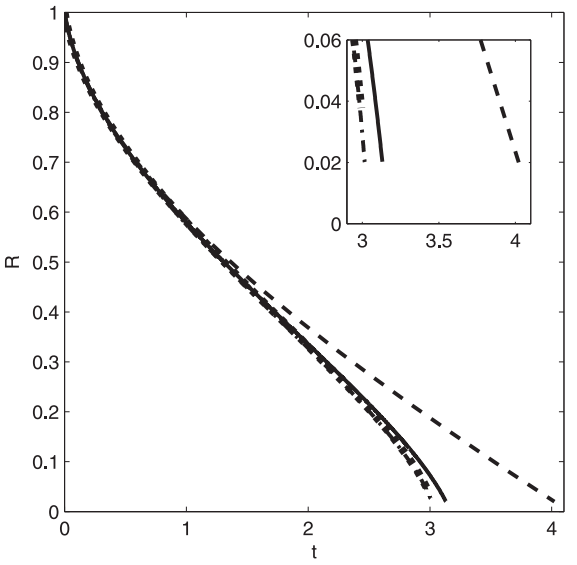

(b) $\beta = 10$, Nu $= 15$.

Fig. 8. Melting front evolution of a cylindrical particle for HBIM in the transformed system (dash-dotted), TIM in the original system (dashed), perturbation (dotted) and numerical (solid) solutions for various β and Nu $= 15$.

The numerical scheme is the one described in Section 3.2.3 but Eq. (67) becomes

$$T_J^{n+1} = (\mathrm{Nu}(1-R^n)\Delta\eta + 1)T_i^{n+1} - T_{i-1}^{n+1} = \mathrm{Nu}(1-R^n)\Delta\eta. \tag{86}$$

5. Conclusion

The goal of this paper was to improve the accuracy of the HBIM applied to Stefan problems in spherical and cylindrical geometries. To do this we analysed the standard form and the optimised form (TIM), in the original and a transformed co-ordinate system, subject to fixed temperature and Newton cooling boundary conditions. The large Stefan number perturbation solution was also calculated to first order since this is the most common way to approximate solutions to Stefan problems. The accuracy was determined by comparison of the predicted melt front position with a numerical solution for two values of the Stefan number $\beta = 1, 10$. The upper limit for β was chosen since it is a typical maximum value for practical melting problems [32].

First we considered melting due to a fixed temperature boundary condition. For the spherical problem all solutions in the original domain were inaccurate for small β. For large β only the perturbation solution was accurate. However, when the temperature variable was changed to $u = rT$ the solutions improved in accuracy. In particular the TIM gave the most accurate solutions for the β values tested. Even when $\beta = 10$, when we expect the perturbation solution to have an accuracy of $O(10^{-2})\%$ the TIM was significantly more accurate. The expression for the temperature with the fixed temperature boundary condition takes the form

$$u = a\left(\frac{r-R}{1-R}\right) + b\left(\frac{r-R}{1-R}\right)^n, \tag{87}$$

where $b = 1 - a$. For the standard HBIM $n = 2$. For the TIM $n \in [1.55, 1.65]$ varies slightly with β. However, choosing the average value $n = 1.6$ provides more accurate solutions than the other methods. Consequently when studying spherical Stefan problems, with a fixed temperature boundary condition we recommend transforming the temperature variable $T = u/r$ where u is given by (87) and $n = 1.6$.

With a Newton cooling condition the conclusions are similar. Firstly, the temperature must be transformed to $u = rT$. The relation between a and b is more complex and with the TIM the exponent varies with both β and $\mathrm{Nu} = hR_0/k$. For small Nu we found good accuracy with the average $n = 1.92$. For larger Nu (here we tested Nu$= 15$) we found a smaller value $n = 1.65$, which is obviously tending to the fixed temperature limit $n = 1.6$ (corresponding to Nu $\to \infty$).

In the case of cylindrical symmetry the results were not so satisfactory. Firstly, the temperature transformation was of no use, instead we used a boundary fixing transformation, which complicated the governing heat equation. Secondly, the TIM proved too complex to be of practical use or appeal. Thirdly, in general accuracy was poor for both boundary conditions.

From this part of the study it is difficult to make a conclusive statement. When $\beta = 1$, for a fixed temperature boundary condition the TIM works best in the original system, for the cooling condition it is more accurate than the HBIM and perturbation calculated in the transformed system. For large β it is the worst, while the perturbation is reasonably accurate for the values of Nu examined.

In conclusion then, it appears that the TIM can be used with great accuracy in spherically symmetric melting problems, provided the temperature transformation $u = rT$ is employed. In the cylindrical problem the results are less conclusive and different methods work better for different parameter values. In this case it is hard to make a single recommendation. However, it is possible that a different transformation, either of the temperature or co-ordinates, could change this conclusion.

Acknowledgements

HR and TM acknowledge that the research leading to these results has received funding from “la Caixa” Foundation. TM acknowledges the support of a Ministerio de Economía y Competitividad Grant MTM2014-56218-C2-1-P. MM acknowledges the support of CERECAM.

References

[1] T.R. Goodman, The heat-balance integral and its application to problems involving a change of phase, Trans. ASME 80 (1958) 335–342.
[2] L.I. Rubinstein, The Stefan Problem, American Mathematical Society, 1971.
[3] J. Hristov, The heat-balance integral method by a parabolic profile with unspecified exponent: analysis and exercises, Therm. Sci. 13 (2) (2009) 27–48.
[4] A. Kumar, S. Roy, Melting of steel spherical particle in its own liquid: application to cladding, J. Thermophys. Heat Transf. 23 (4) (2009) 762–772.
[5] F. Font, T.G. Myers, S.L. Mitchell, A mathematical model for nanoparticle melting with density change, Microfluid. Nanofluidics 18 (2014) 233–243.
[6] W.H. Qi, Size effect on melting temperature of nanosolids, Phys. B 368 (2005) 46–50.
[7] M.A. Shandiz, A. Safaei, S. Sanjabi, Z.H. Barber, Modeling size dependence of melting temperature of metallic nanoparticles, J. Phys. Chem. Solids 68 (2007) 1396–1399.
[8] F. Font, T.G. Myers, Spherically symmetric nanoparticle melting with a variable phase change temperature, J. Nanoparticle Res. 15 (2013) 2086.
[9] F. Font, S.L. Mitchell, T.G. Myers, One-dimensional solidification of supercooled melts, Int. J. Heat Mass Transf. 62 (2013) 411–421.
[10] A. Sharma, V.V. Tyagi, C.R. Chen, D. Buddhi, Review on thermal energy storage with phase change materials and applications, Renew. Sustain. Energy Rev. 13 (2009) 318–345.
[11] T.G. Myers, J. Low, An approximate mathematical model for solidification of a flowing liquid in a microchannel, Microfluid. Nanofluid 11 (2011) 417–428.
[12] T.G. Myers, J. Low, Modelling the solidification of a power-law fluid flowing through a narrow pipe, Int. J. Therm. Sci. 7 (2013) 127–131.
[13] S.H. Xu, G.T. Fei, Y. Zhang, X.F. Li, Z. Jin, L.D. Zhang, Size-dependent melting behavior of indium nanowires, Phys. Lett. A 375 (2011) 1746–1750.
[14] H.-S. Ren, Application of the heat-balance integral to an inverse Stefan problem, Int. J. Therm. Sci. 46 (2007) 118–127.
[15] S.K. Sahu, P.K. Das, S. Bhattacharyya, A comprehensive analysis of conduction-controlled rewetting by the heat balance integral method, Int. J. Heat Mass Transf. 49 (2006) 4978–4986.
[16] A.S. Wood, A new look at the heat balance integral method, Appl. Math. Model. 25 (10) (2001) 815–824.
[17] M.M. MacDevette, T.G. Myers, Contact melting of a three-dimensional phase change material on a at substrate, Int. J. Heat Mass Transf. 55 (2012) 6798–6807.
[18] E. Vázquez-Nava, C.J. Lawrence, Thermal dissolution of a spherical particle with a moving boundary, Heat Transf. Eng. 30 (5) (2009) 416–426.
[19] J. Caldwell, C.K. Chiu, Numerical solution of one-phase Stefan problems by the heat balance integral method, Part I - Cylind. Spherical Geom. Commun. Numer. Methods Eng. 16 (2000) 569–583.
[20] J. Caldwell, C.C. Chan, Numerical solutions of the Stefan problem by the enthalpy method and the heat balance integral method, Numer. Heat Transf. Part B: Fundam.: Int. J. Comput. Methodol. 33 (1) (1998) 99–117.
[21] J.M. Hill, One-Dimensional Stefan Problem: An Introduction, Longman Scientific and Technical, Essex, 1987.
[22] G.E. Bell, A refinement of the heat balance integral method applied to a melting problem, Int. J. Heat Mass Transfer 21 (11) (1978) 1357–1362.
[23] S.L. Mitchell, An accurate nodal heat balance integral method with spatial subdivision, Numer. Heat Transf. B 60 (1) (2011) 34–56.
[24] F. Mosally, A.S. Wood, A. Al-Fhaid, On the convergence of the heat balance integral method, Appl. Math. Comput. 29 (2005) 903–912.
[25] A.S. Wood, F. Mosally, A. Al-Fhaid, On higher-order polynomial heat-balance integral implementations, Therm. Sci. 13 (2) (2009) 11–25.
[26] J. Caldwell, C.-C. Chan, Spherical solidification by the enthalpy method and the heat balance integral method, Appl. Math. Model. 24 (2000) 45–53.
[27] T.G. Myers, Optimizing the exponent in the heat balance and refined integral methods, Int. Commun. Heat Mass Transf. 36 (2) (2009) 143–147.
[28] T.G. Myers, Optimal exponent heat balance and refined integral methods applied to Stefan problems, Int. J. Heat Mass Transf. 53 (2010) 1119–1127.
[29] S.L. Mitchell, T.G. Myers, Improving the accuracy of heat balance integral methods applied to thermal problems with time dependent boundary conditions, Int. J. Heat Mass Transf. 53 (2010) 3540–3551.
[30] T.G. Myers, S.L. Mitchell, Application of the combined integral method to Stefan problems, Appl. Math. Model. 34 (2011) 4281–4294.
[31] T.G. Myers, S.L. Mitchell, F. Font, Energy conservation in the one-phase supercooled Stefan problem, Int. Commun. Heat Mass Transf. 39 (2012) 1522–1525.
[32] V. Alexiades, A.D. Solomon, Mathematical Modelling of Melting and Freezing Processes, Hemisphere Publishing Corp., 1993.
[33] C.-L. Huang, Y.-P. Shih, A perturbation method for spherical and cylindrical solidification, Chem. Eng. Sci. 30 (8) (1975) 89–906.
[34] T.G. Myers, M.M. MacDevette, H. Ribera, A time-dependent model to determine the thermal conductivity of a nanofluid, J. Nanopart Res. 15 (2013) 1775.
[35] H. Ribera, T.G. Myers, A mathematical model for nanoparticle melting with size-dependent latent heat and melt temperature, Microfluid. Nanofluidics 20 (11) (2016) 147.
[36] B.J. Florio, T.G. Myers, The melting and solidification of nanowires, J. Nanoparticle Res. 18 (6) (2016) 1–12.
[37] N. Sadoun, E.K. Si-Ahmed, P. Colinet, On the refined integral method for the one-phase Stefan problem with time-dependent boundary conditions, Appl. Math. Model. 30 (6) (2006) 531–544.
[38] S.L. Mitchell, T.G. Myers, Application of standard and refined heat balance integral methods to one-dimensional Stefan problems, SIAM Rev. 52 (1) (2010) 57–86.
[39] S.L. Mitchell, M. Vynnycky, Finite-difference methods with increased accuracy and correct initialization for one-dimensional Stefan problems, Appl. Math. Comput. 215 (4) (2009) 1609–1621.
[40] O.P. Layeni, J.V. Johnson, Hybrids of the heat balance integral method, Appl. Math. Comput. 218 (14) (2012) 7431–7444.
[41] S.L. Mitchell, Applying the combined integral method to two-phase Stefan problems with delayed onset of phase change, J. Comput. Appl. Math. 281 (2015) 58–73.